A Next Generation On-Line Enrichment Monitor (OLEM) Prototype

James Ely
Stephen Chadwick
Nikhil Deshmukh
Rodrigo Guerrero
Benjamin McDonald
Riane Stene
Mital Zalavadia

Pacific Northwest National Laboratory
902 Battelle Ave
Richland, WA 99354 USA
E-mail: James.Ely@pnnl.gov

Abstract:

The International Atomic Energy Agency (IAEA) has deployed the On-Line Enrichment Monitor (OLEM) to measure the ^{235}U enrichment of UF_6 gas flowing in header pipes in gaseous centrifuge enrichment plants. A next generation prototype OLEM has been developed to alleviate a challenge with accounting for deposits on the interior of the pipe. Deposits have the same radiometric signature as the UF_6 gas and are indistinguishable in the current OLEM. The current analysis approach estimates the deposit contribution by extrapolation of radiation detector response as a function of the UF_6 gas process, typically a two-step analysis process. Using a modified dual-collimator approach with an array of cadmium-zinc-telluride (CZT) detectors, a next generation OLEM prototype has been built and performance demonstrated in a lab environment. The system provides real-time measurement of the UF_6 gas and deposits separately, potentially increasing precision and reducing analysis time. This next-generation OLEM also is smaller, with about half the size and weight of the current OLEM. This paper will provide an overview of the prototype design and the results of measurements in the lab.

1. Introduction

The International Atomic Energy Agency (IAEA) has developed and deployed an On-Line Enrichment Monitor (OLEM) with the assistance of the US Support Program [1], and the National Nuclear Security Agency's Office of International Safeguards and Nuclear Nonproliferation Research and Development programs. The OLEM measures the ^{235}U enrichment of uranium hexafluoride (UF_6) gas in header pipes in enrichment facilities. The OLEM provides advantages over previous and existing systems in that it is unattended, it is mounted on header pipes outside the centrifuge halls, and it does not use radioactive sources.

The OLEM consists of gamma-ray detectors (thallium-doped sodium iodide [NaI]), a pressure transducer, and a thermocouple, along with associated electronics, computer, and housing. The NaI detector measures the gamma-ray emissions from uranium in an UF_6 header pipe. The background subtracted counts in the 186 keV region of the gamma-ray spectrum are proportional to the ^{235}U in the field of view of the detector, because ^{235}U emits a 186 keV

gamma-ray during radioactive decay. The pressure and temperature (thermocouple) measurements allow determination of the total uranium by the UF_6 equation of state using the empirical Weinstock approach [2]. These three measurements (gamma-ray counts in the region of interest, pressure, and temperature) are combined with calibration constants to produce an enrichment value.

The background in the 186 keV region is a combination of two parts; one background arises from higher energy gamma-rays that deposit part of their energy in the detector, either due to external down-scattering or Compton scattering in the detector material itself. This forms a continuum background under the 186 keV peak. The sources are higher-energy internal sources (such as ^{238}U in wall deposits or the UF_6 gas) or external sources, such as those from the environment (concrete floors or walls) or nearby UF_6 cylinders or other radioactive sources in the view of the OLEM detector.

The second background contribution, which contributes to the 186 keV peak itself, is from ^{235}U in wall deposits of the pipe. Uranium deposits contain ^{235}U and emit a 186 keV gamma-ray which contributes to the ^{235}U peak, the same as the UF_6 gas flowing in the pipe. External ^{235}U contributions to the 186 keV peak are insignificant as the detector is shielded. The deposits are uranium solids that form on the pipe walls and arise from several processes. The UF_6 chemically interacts in new pipes with the wall material and creates deposits (passivated surface) or interacts with other materials (water vapor for example) and creates solid material, typically UO_2F_2, that lines the pipe. Another contribution is from radioactive decay in which the progeny ion becomes attached to the wall. The deposit background is challenging to quantify and subtract out as it is indistinguishable from the gas contributions in the 186 keV region (see Figure 1).

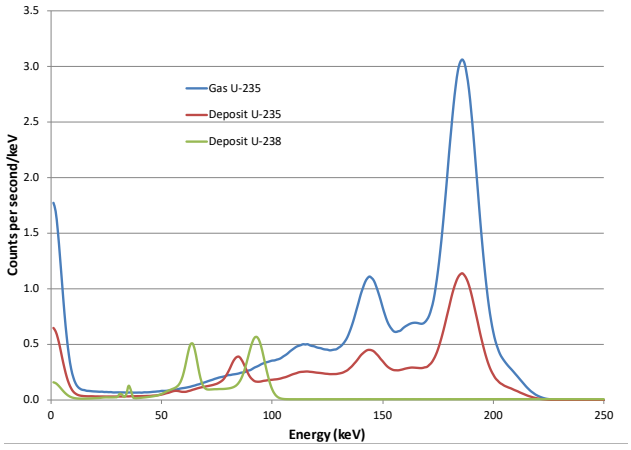

Figure 1. Example simulated energy spectra in a NaI detector of UF_6. The blue line represents the ^{235}U from the gas, the red line is ^{235}U wall deposits, and the green line is ^{238}U from wall deposits.

The primary approach to quantifying the deposit background is to monitor the gamma-ray count rate as a function of the UF_6 pressure or density, which has a linear proportional relationship. By extrapolating the count rate to zero UF_6 pressure, one can estimate the deposit contribution. This is shown in Figure 2. This approach works well if the UF_6 pressure changes over a fairly large range to constrain the extrapolation and minimize the uncertainty. However, this requires several post-analysis steps, first to estimate the deposits for an ensemble of measurement, the second to calculate the enrichment for each measurement. And,

the pressure changes need to be collected over a period of time, during which the deposits could be changing. The assumption is the deposits do not change over the time period when the pressure variations are collected. A real-time measurement of the deposits would improve the measurement precision and reduce the post-analysis of the data.

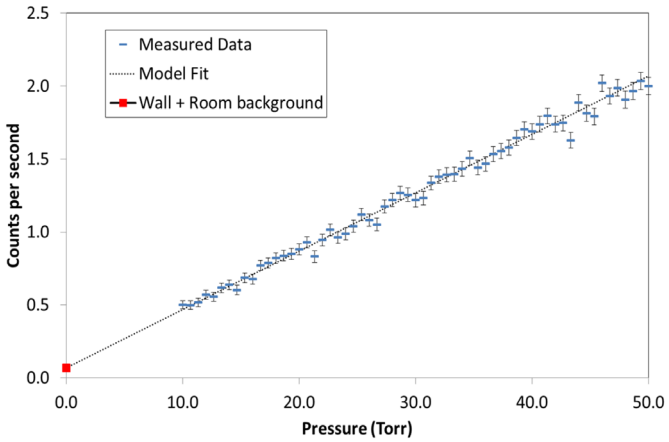

Figure 2. The gamma-ray counts versus pressure for simulated data, illustrating the extrapolation to zero pressure. The y-axis intercept provides the wall deposit (and room background) contribution to the count rate.

There are approaches to measure the deposit contributions in real time using a dual collimator approach [3]. This can be accomplished with either a single detector and a rotating collimator [4] or with multiple detectors [5, 6]. The next generation OLEM uses arrays of cadmium-zinc-telluride (CZT) detectors with two types of collimators to measure gas and deposit contributions in real-time. This approach avoids rotating collimators and aims to improve the enrichment measurement precision while reducing the weight and footprint of the system.

2. Dual Collimator Approach

The dual collimator approach makes measurements with two collimators: one optimized to measure relatively more UF_6 gas than deposits, the other optimized to measure relatively more deposits. By taking measurements with two different collimators, and knowing the detection efficiency for each, the contribution of the gas and deposits can be calculated.

Here we follow the formulism developed by Close and Pratt [3] for the two positions of the collimator, either parallel (∥) or perpendicular to the direction of the gas flow in the pipe (⊦) and the equations therefrom which provide either the gas (G) or the deposits (D) contributions:

$$G = \frac{U\parallel - \beta U\vdash}{\alpha - \beta}, \quad D = \frac{\alpha U\vdash - U\parallel}{\alpha - \beta}$$

where ($U\vdash$) is total perpendicular count rate, (U∥) is the total parallel count rate, and α and β are constants and are the efficiency ratios between the perpendicular and parallel collimator geometry.

The uncertainty on the gas count rate in the 186 keV peak can be determined using variance propagation in the first order Taylor expansion, here assuming no covariance:

$$\sigma_G^2 = \left[\frac{U\parallel - \beta U\vdash}{(\alpha-\beta)^2}\right]^2 \sigma_\alpha^2 + \left[\frac{U\parallel - \alpha U\vdash}{(\alpha-\beta)^2}\right]^2 \sigma_\beta^2 + \left[\frac{\beta}{(\alpha-\beta)}\right]^2 \sigma_{U\vdash}^2 + \left[\frac{1}{(\alpha-\beta)}\right]^2 \sigma_{U\parallel}^2$$

3. Modelling and Simulation

To explore the possibility of using detector arrays, models of the pipe, gas, and deposits were developed along with detectors and simulations performed using the radiation transport code Monte Carlo N-Particle (MCNP 6.2) [7]. The modeling and simulation results were presented at a previous annual meeting [8] and will not be covered in detail here.

The simulations provided estimation of the efficiencies for the gas and deposit contributions and, using the formulation described in the previous section, the gas contribution could be estimated. The uncertainty on the gas contribution, or precision of the measurement, was used as the metric to explore the parameter space and to optimize a design. Improving the precision or minimizing the uncertainty on the enrichment measurement was the main goal of the initial modeling and simulation as well as optimizing the detector and collimators.

The MCNP simulation results were used in Microsoft EXCEL to perform scaling variations with respect to the number of detectors, enrichment, pressure, gas-to-deposit ratios, and averaging time, and to calculate the estimated relative uncertainty associated with the gas counts in a system configuration.

The source was separately modelled for the UF_6 gas and for the wall deposits. The UF_6 gas was assumed to be UF_6 with 5% ^{235}U enrichment. Only ^{235}U gamma emission was included because ^{238}U decay is not significant in the UF_6 gas stream. The wall deposit source was modelled as a thin (10 microns) radioactive layer of UO_2F_2 on the inside of the pipe. For the ^{235}U in the deposits, the gamma-ray emission of the ^{235}U itself is included, with the energies described above, along with emissions from the progeny ^{231}Th, which has a half-life of 1.063 days. For the ^{238}U chain in the deposits, the main emissions are from the decay progeny ^{234}Th (24.1-day half-life) and ^{234m}Pa (1.17 min half-life).

Three different pipe models were developed: 2-inch diameter, 4-inch and 6-inch diameter, all Schedule 40. The material was modeled as aluminum and, also as stainless steel as a variation. The pipes were modelled as short sections of pipe, each 50 cm long as shown in Figure 3. This length is sufficient to allow for entire coverage of the field of view of the collimated detectors.

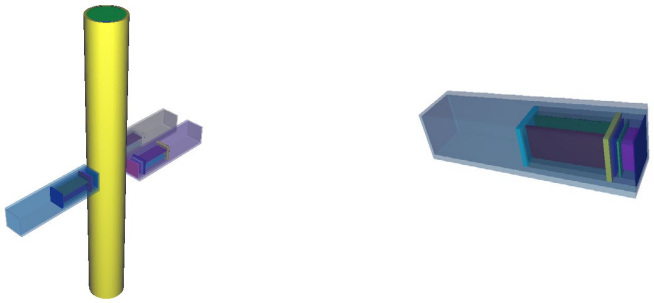

Figure 3. Screen capture of the 3D rendering of the model showing the 2-inch diameter stainless steel pipe and three detector modules (left) and a single detector model (right) with the CZT crystal at the end.

The detector models used the Ritec CZT model µSpec1500 as the basis detector, shown in Figure 3 (right). The detector material was modelled as a simple cube of CZT of 15 × 15 × 7.5 mm^3. The detector was enclosed in a 3 mm thick tungsten shield of 150 × 33 × 33 mm^3.
The collimator has sufficient length to allow effective collimation even when the detector was moved back from the end.

The detector array was modelled as three detectors with the same collimator. There was one detector centered on the pipe, and two located near the edge of the pipe, where the position of the detector would provide the difference in relative efficiency between the gas and deposits.

Additional detectors were accounted for in the analysis by multiplying either a central detector or an edge detector instead of simulating all possible configurations in MCNP. After initial explorations, a different collimator type, a V-shaped one (see Figure 4), was used to provide a better relative efficiency for the deposits, and the detector was relocated to the center of the pipe.

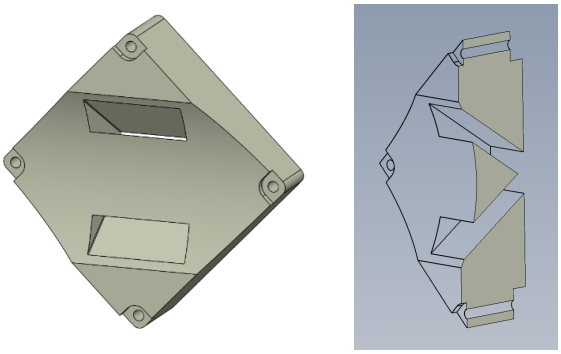

Figure 4. Design of the triangular collimator showing the opening that focuses on the sides of the pipe. Left shows the pipe side of the collimator with the rounded shape to better match the round pipe; right shows a cutaway of the collimator.

The simulation results consisted of the energy deposition in the CZT detectors. The resulting spectra were post-processed using a set of functions to describe and simulate the detector response [9]. This post-processing step broadens the energy deposition peaks from MCNP and adds a low-energy tailing on the peaks due to incomplete charge collection of CZT. The region around the 186 keV peak was summed and the counts ratioed to the number of generated particles to determine efficiencies.

The relative uncertainty in the gas measurement was calculated with regard to many parameters including pipe size, pipe material, number of detectors, detector standoff distance, UF_6 gas pressure, deposit thickness, enrichment, and measurement time. When varying one parameter, the other parameters were held fixed. For many of the parameters explored, including the number of detectors, enrichment, pressure, gas-to-deposit ratios, and averaging times, the relative uncertainty followed a square root scaling. This was expected as only statistical uncertainty was included and is the square root of the counts. For example, the uncertainty as a function of enrichment, shown in Figure 6, illustrates this square root behavior.

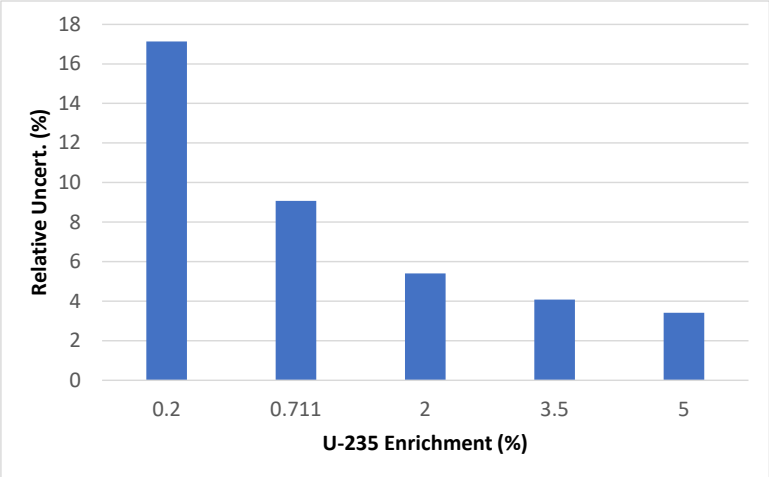

Figure 5. Simulated relative uncertainty of the enrichment measurement as a function of ^{235}U enrichment for the 2-inch diameter pipe with the nominal parameter set.

The smallest pipe size has the largest uncertainty which increases when switching from aluminum to stainless steel, as the attenuation reduces the signal reaching the detectors. For these reasons, the most challenging case for optimization is the smallest pipe with stainless steel.

Two parameters did not have a square root scaling: the stand-off distance and the slit width of the V-shaped collimator. In both of these cases, when the stand-off distance was minimized or the slit width maximized, the efficiency was the largest, but the differentiation between the gas and deposits was not optimal. At large stand-off distances or narrow slit widths, the efficiency was small, but the differentiation was the largest. With the efficiency and differentiation competing with each other, the optimal was in the middle. For the stand-off distance, this is 10 mm, and the slit width is 4 mm.

5. Benchtop Prototype

Based on model and simulation results, a benchtop prototype was designed and built. An image of the system and collimators is shown in Figure 6. This prototype will be useful to validate the simulations, and to demonstrate the capability of this approach. The prototype incorporates three pairs of detectors for a total of six detectors, chosen to provide enough detectors to be able to vary analysis parameters and compare to simulation results, while minimizing the cost. Depending on the level of sensitivity needed, fewer or additional detector could be used.

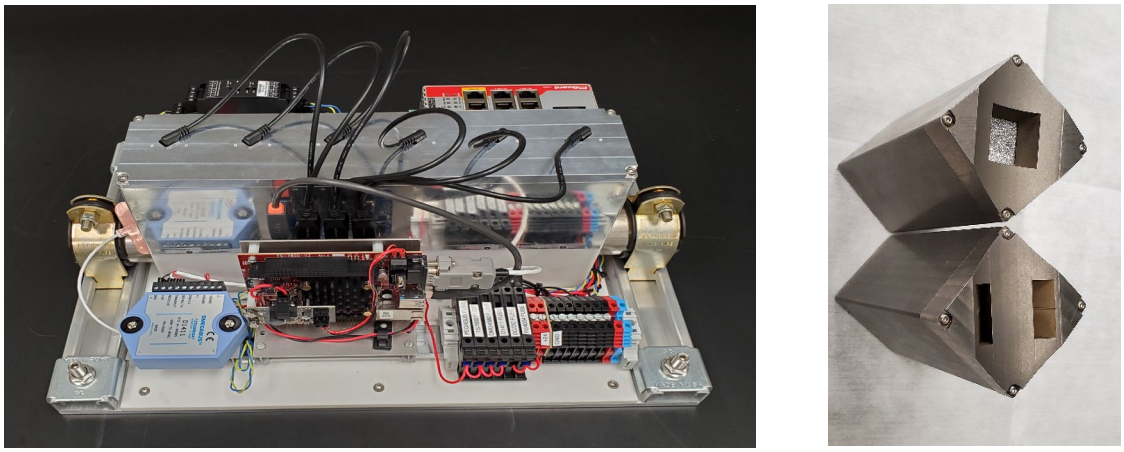

Figure 6. Left: assembled benchtop prototype with the six detector locations on top of the pipe. Right: end view of the two collimator types.

The prototype incorporates the V-shaped collimator for three of the detectors and square collimator for the others. The detectors were arrayed in a line along the pipe for a simple layout scheme, and the electronic components arrayed along the side of the detector housing. Although the design could be made more compact, this benchtop prototype system has about ½ the volume of the current OLEM system, and about ½ the weight.

The design of this next-generation OLEM took into account the current OLEM electronics and computer and used the same components to allow maximum compatibility with the existing OLEM for maintenance and spare components. The detectors are different, being multiple CZT rather than a single NaI detector, and required the addition of a 6-port USB hub (see Figure 7). The hardware virtual private network (VPN) was also upgraded to the current IAEA usage, and the computer was upgraded to the next version of the same model. All other electronic components are the same as the current OLEM.

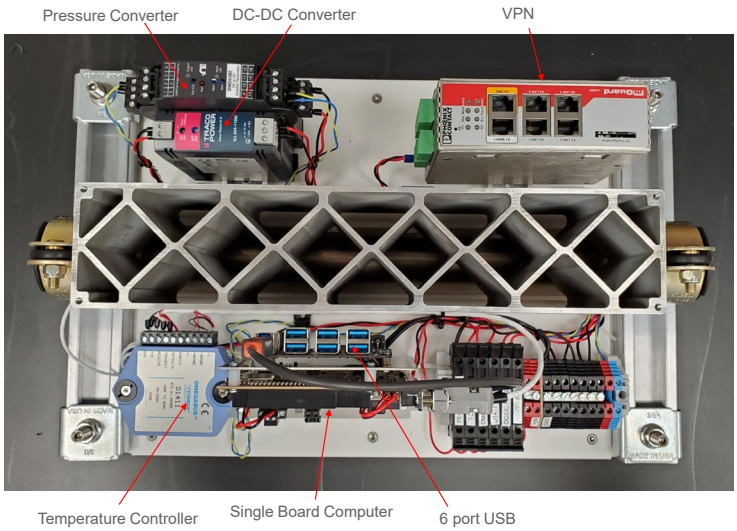

Figure 7. Next generation OLEM without the detectors showing the electronic components.

To accompany the hardware, a suite of initial prototype software was developed. A data acquisition software resides on the single board computer to collect data at a user-selected time scale. The data acquisition software includes a detector data acquisition module for each detector, which makes adding or subtracting detectors straightforward, if needed, in the future. The detector measures individual events as pulses and the pulse heights are input to on-board multi-channel analyzer resulting in a pulse height spectrum that is read from the detector. This pulse height spectrum is proportional to the energy deposited in the detector and once properly calibrated becomes an energy spectrum. The pressure and temperature are input into conditioning electronics and read into the single board computer as voltages and temperature (in Celsius). The pressure and temperature can be read out at a higher frequency than the detector spectra, to support data quality checking. The data acquisition software collects the data from the six detectors, and pressure and temperature conditioning modules and writes the data to files when the detector spectra collection is completed. The data is stored locally on the single board computer and could be copied through the hardware VPN to other locations.

A prototypical analysis software has been developed to analyze the data and calculate the enrichment values. The analysis software reads in the datafiles, and based on a user-specified analysis time, sums the data appropriately. The detector spectra are fit with a peak fitting software from the IAEA called the General Enrichment Meter, which is a generalized version of the NaIGEM code [10] to include CZT as well as other detector types. The GEM provides the estimated peak counts in the 186 keV region and using the data from the two collimators and the efficiencies from the simulation, the emissions from the UF_6 gas can be calculated. The enrichment is then calculated using the average pressure and temperature values and the equation of state along with a proportionality constant. A proportionality constant has to be determined from the known enrichment value during calibration, which can be from a destructive analysis sample, for example. The analysis software writes the enrichment and uncertainty values to a results file, along with the values used in the analysis steps. In addition to the analysis software, a prototype data viewer has been developed to plot analysis results as a function of time. The viewer may plot any of the values in the results file, and also as a function of other parameters to examine potential correlations.

Experiments were performed and additional experiments are underway to evaluate the performance of the next generation OLEM and validate the simulation results. A static pipe

testing system for UF_6 was developed that allows for deposit development with UF_6 gas flowing through the pipe. Initially, long duration measurements were made with depleted uranium UF_6 in the pipe to validate the simulated efficiency. This is shown in Figure 9 for the square collimator (upper points and line) and the V-shaped collimator (lower points and line). Since the pressure and temperature of the gas, and the pipe volume are known, the efficiency can be calculated from the observed counts in the 186 keV peak. The measured efficiency for the square collimators is approximately 25% lower than the simulated efficiency. However, the efficiency from the measurements for the V-shaped collimators is consistent with the simulation. In further investigation of the results further, it was found that the model for the simulation is not consistent with the as-built V-shaped collimator, where the slit width was not the same. The model is being updated and the analysis will be repeated. And the experiment will need to be repeated with low enriched UF_6. Validating the deposits is not as straightforward, as there is not an easy method to determine the deposit thickness (on the order of a micron or so).

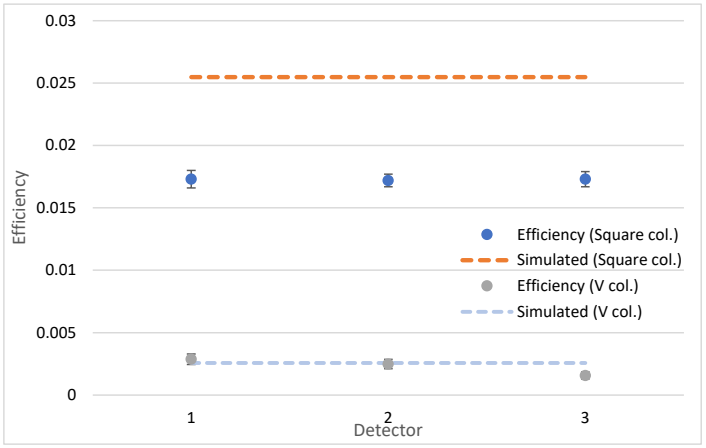

Figure 8. Measured and simulated efficiencies for the square collimator (upper points and line) and for the V-shaped collimator (lower points and line).

During the development and initial testing of the static pipe, depleted uranium in the form of UF_6 gas was used. Humid air was used to convert a small amount of UF_6 into deposits, and this process repeated until the deposit signal on the OLEM was comparable to the UF_6 gas itself. The depleted uranium does not have a significant signal, therefore, an 18% enriched UF_6 gas was used in a follow experiment to increase the signal. This experiment with 18% UF_6 gas was conducted at various pressures with the depleted deposit. Initial data analysis has been conducted, with unexpected observations, where it appears the deposits increased during the experiment. An example of the data is shown below in Figure 9 for a four-hour analysis period for the detectors with the square collimator. The post-experiment counts without UF_6 gas are about two times larger than the pre-experiment counts, exhibiting a bi-modal distribution at zero pressure, and a non-linear distribution as a function of pressure. This behavior is not understood, since no air was introduced into the system and there should not have been any deposits created from the 18% UF_6. Possibilities include an unknown small leak in the system, or UF_6 de-sublimating onto the walls during the experiment. Additional analysis is underway and plans to repeat the experiment with additional zero pressure measurements taken in-between each UF_6 pressure value.

Depleted UF_6 was used during the initial deposit formation to avoid loss of enriched uranium when optimizing the deposition process. The next planned experiment after understanding the observed increase in deposits during the 18% UF_6 experiment will be to develop low-enriched

uranium (LEU) deposits and evaluate the OLEM with both LEU deposits and UF_6. As with the previous experiments, measurements of UF_6 only, deposits only, and both will be made. When the combined measurements are performed, the UF_6 pressures will be varied to observe the dependence on the total gas density.

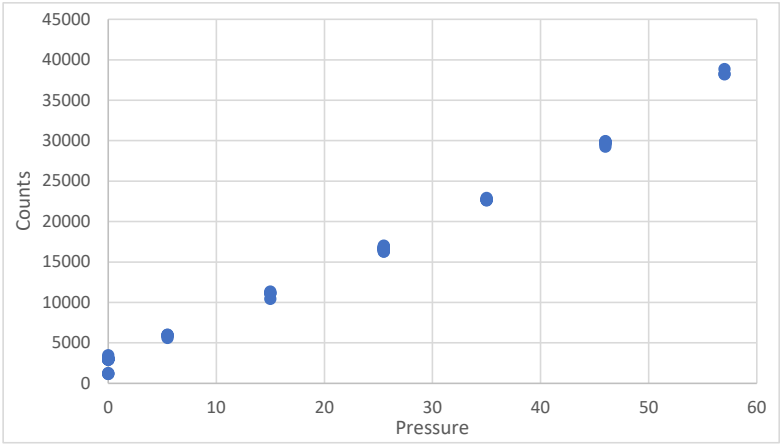

Figure 9. Counts in the CZT detectors with the square collimator with a 4 h analysis period for the 18% UF6 experiment as a function of UF6 gas pressure.

6. Conclusions

A next generation OLEM prototype has been designed and built. This prototype uses an array of CZT detectors and two different collimators to measure the ^{235}U contribution and deduce the UF_6 gas enrichment level. The research started with modeling and simulation to optimize a design and based on the results, a prototype system was built. A static test pipe system was developed and used for testing and evaluation of the prototype OLEM with deposits and gas. Initial experiments have been conducted with depleted uranium deposits and gas. Initial comparison of the data to the simulation is promising but the model needs to be updated to reflect the as-built dimensions. Additional experiments are planned to further validate and understand the prototype performance.

The next generation OLEM has shown, through modeling and initial experiments, to be able to measure UF_6 gas and wall deposits using a CZT detector array with two collimator types. This allows extraction of the UF_6 gas contribution from the measurement and hence, the enrichment value. This approach will reduce the uncertainty in the enrichment measurement and the need for post-processing analysis. In addition, the next generation OLEM has a smaller form factor of about one-half the size and weight of the current OLEM.

5. Acknowledgements

The work presented in this paper was funded by the National Nuclear Security Administration of the Department of Energy, Office of International Nuclear Safeguards.

7. References

[1]https://www.iaea.org/newscenter/news/new-iaea-uranium-enrichment-monitor-verify-iran%E2%80%99s-commitments-under-jcpoa; https://www.energy.gov/nnsa/articles/olem-nnsa-capability-strengthens-global-nuclear-safeguards-mission

[2] DeWitt, R. “Uranium Hexafluoride: A Survey of the Physiochemical Properties,” GAT-280, Portsmouth Gaseous Diffusion Plant. 1960.
[3] Close, D. A., J. C. Pratt, and H. F. Atwater, “Development of an Enrichment Measurement Technique and its Application to Enrichment Verification of Gaseous UF6,” Nuclear Instruments and Methods A 240, 398. 1985.
[4] Close D. A, J. C. Pratt. “Improvements in Collimator Design for Verification of Uranium Enrichment in Gaseous Centrifuge Header Pipes of Diameter 4.45 cm and 10.16 cm,” Nuclear Instruments and Methods in Physics Research A257, 406-411. 1987.
[5] Packer T. W., *et al.*, “Measurement of the Enrichment of Uranium in the Pipework of a Gas Centrifuge Plant,” Proc. 6th Annual Symposium on Safeguards and Nuclear Material Management, ESARDA, Venice, Italy, p. 243. 1984.
[6] Favalli, A. *et. al.*, “Multi-detector system approach for unattended uranium enrichment monitoring at gas centrifuge enrichment plants” Nuclear Instruments and Methods in Physics Research A877, 138-142. 2018.
[7] Werner, C.J. (editor), "MCNP User’s Manual - Code Version 6.2", Los Alamos National Laboratory, report LA-UR-17-29981. 2017.
[8] Ely, J., R. Guerrerro, B. McDonald, and M. Zalavadia, “Advancing the On-Line Enrichment Monitor (OLEM) Capability”, Proc. of the Annual Meeting of the Institute of Nuclear Materials Management, virtual, 2021. PNNL-SA-163745.
[9] Mortreau, P., R Berndt., “Characterization of cadmium zinc telluride spectra - application to the analysis of spent fuel spectra”, Nuclear Instruments and Methods in Physics Research A458, 183-188. 2001.
[10] Gunnink, R., “NaIGEM Uranium Isotopic Analysis Code for NaI and LaBr3 Detectors, Version 2.1. 4 [software]”. 2017.